

Review

# Advancements on Ultrasonic Degradation of Per- and Polyfluoroalkyl Substances (PFAS): Toward Hybrid Approaches

Olalekan Simon Awoyemi <sup>1,2</sup> , Ravi Naidu <sup>1,2</sup> and Cheng Fang <sup>1,2,\*</sup>

<sup>1</sup> Global Centre for Environmental Remediation (GCER), School of Environmental and Life Sciences, University of Newcastle, Callaghan, NSW 2308, Australia

<sup>2</sup> CRC for Contamination Assessment and Remediation of the Environment (CRC CARE), University of Newcastle, Callaghan, NSW 2308, Australia

\* Correspondence: cheng.fang@newcastle.edu.au

**Abstract:** Per- and polyfluoroalkyl substance (PFAS) contamination has emerged as a significant environmental concern, necessitating the development of effective degradation technologies. Among these technologies, ultrasonication has gained increasing attention. However, there is still limited knowledge of its scale-up or on-site applications due to the complexity of real-world conditions and its high energy consumption. Herein, we provide an overview of recent advancements in the ultrasonic degradation of PFAS toward hybrid technologies. This review contains information regarding the physical and chemical properties of PFAS, followed by an exploration of degradation challenges, the mechanisms of ultrasonication, and recent experimental findings in this field. The key factor affecting ultrasonication is cavitation intensity, which depends on ultrasonic frequency, power density, and PFAS structure. Its main advantages include the generation of reactive species without chemicals and the compatibility with other degradation technologies, while its main disadvantages are high energy consumption and limited applications to liquid-based media. We also highlight the integration of ultrasonication with other advanced oxidation processes (AOPs) to create hybrid systems for enhanced degradation of PFAS in order to significantly improve PFAS degradation efficiency, with enhancement factors ranging between 2 and 12. Finally, we discuss prospects for scaling up the ultrasonic degradation of PFAS and address the associated limitations. This review aims to deepen the understanding of ultrasonication technology in addressing PFAS contamination and to guide future research and development efforts.

**Keywords:** PFAS; sonication; degradation; advanced oxidation process; hybrid



**Citation:** Awoyemi, O.S.; Naidu, R.; Fang, C.. Advancements on Ultrasonic Degradation of Per- and Polyfluoroalkyl Substances (PFAS): Toward Hybrid Approaches. *Environments* **2024**, *11*, 187. <https://doi.org/10.3390/environments11090187>

Academic Editor: Sergio Ulgiati

Received: 18 June 2024

Revised: 26 July 2024

Accepted: 19 August 2024

Published: 30 August 2024



**Copyright:** © 2024 by the authors. Licensee MDPI, Basel, Switzerland. This article is an open access article distributed under the terms and conditions of the Creative Commons Attribution (CC BY) license (<https://creativecommons.org/licenses/by/4.0/>).

## 1. Introduction

Per- and polyfluoroalkyl substances (PFAS) are a group of synthetic chemicals known for their unique properties, including water and grease resistance, thus being widely used in various industrial and consumer products [1]. However, their persistence, bio-accumulative nature, and potential health effects have raised alarms [2]. Consequently, PFAS contamination has emerged as a significant environmental and public health concern [3].

The importance of PFAS remediation cannot be overstated. Effective remediation can remove or reduce PFAS concentrations in soil, groundwater, and surface water, thereby preventing further distribution and minimizing exposure to humans [4]. Various remediations have been developed [5]. Among them, ultrasonication represents a promising degradation technique because it is easy to apply, results in fewer intermediates/by-products, requires less/no chemicals, and is compatible with other techniques [6]. Ultrasonication involves the application of high-frequency sound waves to the contaminated water or soil, creating cavitation of micro-bubbles that implode and generate intense local heating and pressure changes [7]. These effects lead to the degradation of PFAS into less harmful compounds [8–10]. As research and development in ultrasonication progress towards

field and scale-up applications, a unique perspective focusing specifically on the latest advancements in operational parameters and the practical applications of ultrasonication for PFAS degradation is needed to guide further research, as conducted herein.

In this review, we will provide an overview of PFAS contamination in Part 2, discuss the challenges and options of PFAS degradation in Part 3, describe the ultrasonication of PFAS in detail in Part 4, and provide some suggestions in Part 5.

## 2. PFAS Properties and Contamination

Chemically, PFAS are defined by strong carbon–fluorine (C-F) bonds [11], which are among the strongest bonds in organic chemistry because fluorine is the most electronegative element (−4). That is, when fluorine bonds to carbon, it forms the strongest covalent bond, i.e., C-F (or a second one if compared to Si-F, i.e., 485–531 kJ/mol vs. 565 kJ/mol) [12]. This contributes to their exceptional chemical stability and resistance to degradation in nature. The big size of fluorine (compared to hydrogen) and its high electronegativity make the C-F bond unique [5,13]. For example, the low polarizability of C-F bonds gives rise to intermolecular interactions or Van der Waals interactions weaker than hydrogen–carbon (C-H), which leads to decreased boiling points of PFAS in Figure 1a. The larger size of fluorine than hydrogen leads to increased density of PFAS in Figure 1b. Both demonstrate the properties and uniqueness of PFAS.

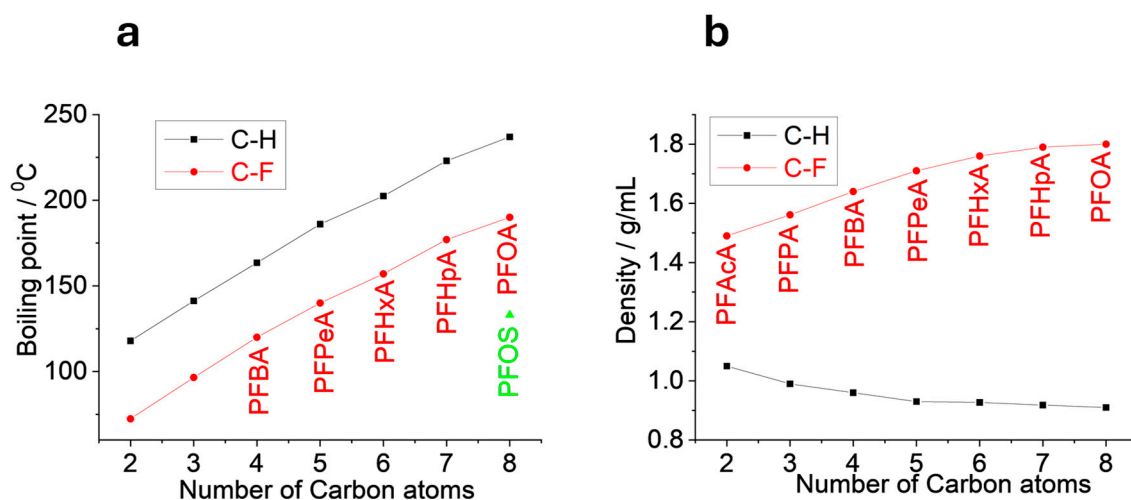


**Figure 1.** Boiling point/temperature (a) and density (b) comparison between the C-F and C-H skeletons for PFCAs and similar compounds. For comparison, the boiling point of PFOS has also been added in (a). The acronyms of PFAS are listed in Table S1 (Supporting Information), and all data were collected from websites, such as indexed Google.

As said, PFAS have been widely used in different applications. Consequently, PFAS are globally detected, including the Arctic [14], dated snow-cores from high mountain glaciers on the Tibetan Plateau [15], and Australian Pinnipeds [16]. Additionally, PFAS are found in cosmetics/personal care products [17], which are examples of non-point sources. Beyond those non-point sources, previously used aqueous film-forming foam (AFFF) on sites can lead to point sources [18].

The ban on perfluorooctanoic acid (PFOA) and perfluorooctane sulfonic acid (PFOS) dating back to the early 2000s has led to the use of various alternatives, such as short chains of perfluoroalkyl carboxylic acids (PFCAs) and perfluoroalkyl sulfonic acids (PFSAs), like perfluorobutane sulfonic acid (PFBS) and perfluorobutanoic acid (PFBA); perfluoro-2-propoxypropanoic acid (GenX); 6:2 fluorotelomer sulfonate (FTSA); polyfluoroalkyl phosphate diesters (diPAPs); and perfluorinated sulfonamidoacetic acids (FOSAAs) [19]. Some of them, such as diPAPs and FOSAAs, are considered as PFAS precursors (are difficult or unable to be monitored quantitatively) as they can degrade into other perfluorinated

substances of PFAS that can be quantitatively monitored. Most of those PFAS precursors or alternatives cannot be effectively and quantitatively detected, either due to the absence of the standard or the testing protocol issue. The non-fluoro part in the precursors can be degraded in the environment to release the detectable PFAS gradually and eventually. That is, the detection and remediation of PFAS has kinetics and thermodynamics, resulting in the remediation challenge.

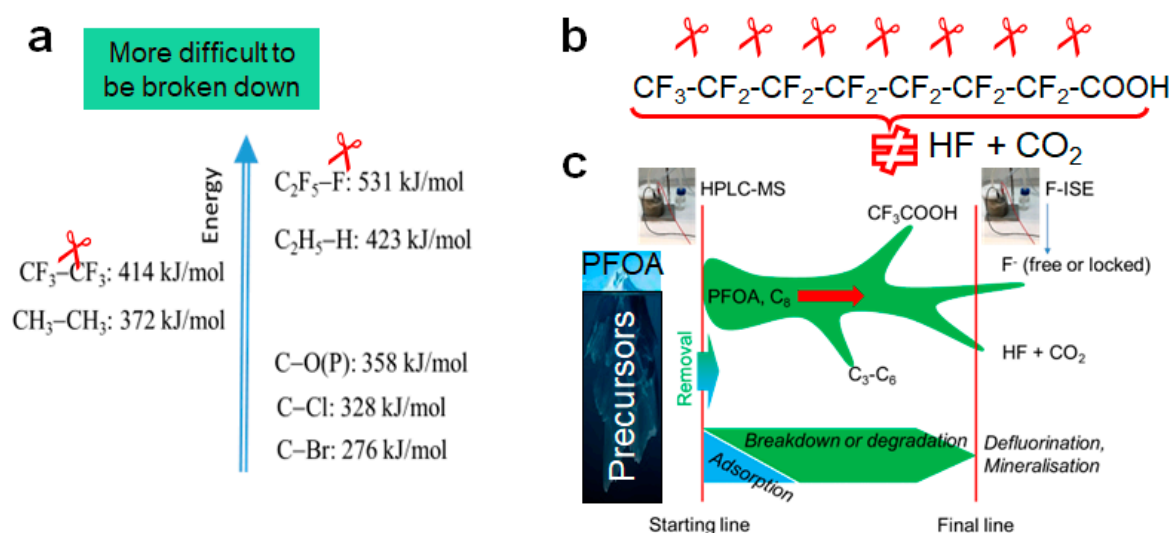
Recently, the Environmental Protection Agency (EPA) of the United States of America (USA) designated two PFAS hazardous substances (PFOA and PFOS with their salts and structural isomers) under the Comprehensive Environmental Response, Compensation, and Liability Act (CERCLA), also known as the Superfund law [20]. The designation of PFOA and PFOS is largely associated to the substantial evidence that they may cause a severe danger to the health and welfare of humans and the environment [20]. The proposed new limit is 4 ppt (part per trillion) for PFOA and PFOS, with an exposure limit in drinking water [21]. This low level of regulation also poses a degradation challenge.

### 3. Remediation and Degradation

PFAS remediation can be categorized as removal and degradation. Removal methods, such as sorption using granulated activated carbon (GAC), reverse osmosis, and nanofiltration, are effective at separating PFAS from water or soil but do not break down the compounds [10]. Instead, they transfer PFAS from one medium to another, leading to the accumulation of PFAS in the environment or in treatment plants, necessitating further treatment toward eventual degradation to effectively mitigate the risk. Unfortunately, the chemical stability of PFAS poses a significant challenge for the degradation of the C-F skeletons, as detailed below.

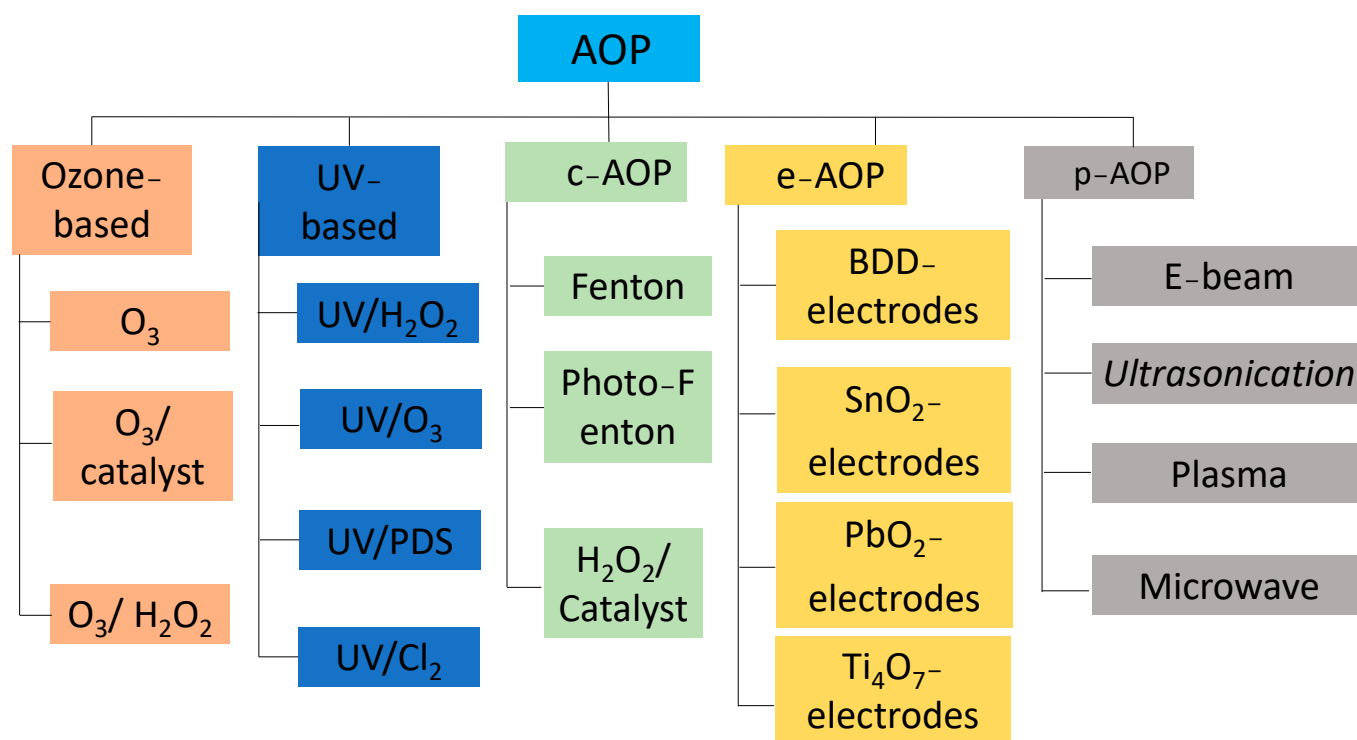
#### 3.1. Degradation Challenges

Figure 2 shows the influence of the C-F bond on PFAS degradation. In (a), the high energy of the covalent bond of C-F renders the degradation challenge. Specifically, the breakdown of the  $\text{CF}_3\text{-CF}_3$  bond is more energetically favorable than that of the  $\text{C}_2\text{F}_5\text{-F}$  bond (414 kJ/mol vs. 531 kJ/mol) [22].



**Figure 2.** Degradation processes of PFAS including the strength of the covalent bonds (a), the degradation sub-steps (b), and the pathway (c). In (c), HPLC–MS (high–performance liquid chromatography–mass spectrometry) monitors PFAS; F–ISE (fluoride–ion selective electrode) measures the concentration of released fluorine as an end product [23], with permission. Copyright 2024 Elsevier.

In Figure 2b, the breakdown of a single bond marks only the initial step in the mineralization process, which necessitates numerous additional sub-steps to achieve degradation to the end products, such as hydrogen fluoride (HF) and carbon dioxide (CO<sub>2</sub>). In (c), different monitoring approaches, such as tracking the initial PFOA with high-performance liquid chromatography–mass spectrometry (HPLC–MS), or monitoring the end product HF with a fluoride–ion selective electrode (F–ISE), can yield disparate results, influencing remediation performance. Additionally, during the degradation process of PFAS exemplified by PFOA, some intermediates may escape from the system, complicating mass balance, such as by monitoring the amount of fluorine. The mass balance might become worse through mechanisms like adsorption or evaporation. The presence of unknown PFAS compounds in the “initial PFOA”, possibly originating from PFAS precursors, further exacerbates the mass balance, especially concerning real environmental samples. Currently, PFAS degradation techniques encompass various advanced oxidation processes (AOPs) and non–AOPs. Studies on various AOPs, such as those presented in Figure 3 for PFAS degradation, have been experimented [24–26] and extensively reviewed in [27–29]. Therefore, in the following sections, we brief non–AOP technologies that have been employed to destroy PFAS and then focus on the ultrasonic degradation of PFAS.



**Figure 3.** Classification of different AOPs. Ozone (O<sub>3</sub>) can be enhanced by a catalyst and hydrogen peroxide (H<sub>2</sub>O<sub>2</sub>). Similarly, UV can also be enhanced by H<sub>2</sub>O<sub>2</sub>, peroxydisulfate (PDS), or chlorine (Cl<sub>2</sub>). C–AOP means catalytic AOP with help from the Fenton reaction, which can be activated by photo or accelerated by catalysis, for example, with H<sub>2</sub>O<sub>2</sub>. Electrochemical AOPs (e–AOPs) can employ electrodes, including BDD (boron-doped diamond), tin (IV) oxide (SnO<sub>2</sub>), lead (IV) peroxide (PbO<sub>2</sub>), and Magneli phase (Ti<sub>4</sub>O<sub>7</sub>). P–AOP (physical AOP) contains E-beam, as mentioned below, ultrasonication, which is the main focus of this review, plasma, microwave, etc. This figure is based on [30], with permission. Copyright 2018 Elsevier.

### 3.2. Degradation Option: Non–AOP

Innovative non–AOP methods have been reported, including thermal degradation, ball milling, and E–beam, as discussed herein.

### 3.2.1. Thermal Degradation

A high temperature is needed for PFAS mineralization, such as 600–1000 °C [31], 350–650 °C [32], or 150–550 °C [33]. Interestingly, a sodium hydroxide-mediated defluorination method was developed to effectively destroy concentrated PFCAs within 24 h at 120 °C, achieving high fluoride ion recovery (78–100%) and minimizing fluorinated by-products, with potential applicability to other PFAS [34]. Recently, 2D Gaussian modeling has been used to visualize degradation kinetics, optimizing the process by considering both time and temperature simultaneously, unlike traditional 1D methods [35]. It is crucial to capture and treat hazardous by-products like HF because the by-products generated can be toxic in potential.

### 3.2.2. Ball Milling

Ball milling is a mechanochemical technique that degrades organics through mechanical crushing or milling to generate high temperatures in specific areas [36,37]. For PFAS degradation, milling agents like alumina ( $\text{Al}_2\text{O}_3$ ), potassium persulfate ( $\text{K}_2\text{S}_2\text{O}_8$ ) [37], and potassium hydroxide (KOH) [38] are used. Co-milling agents are crucial, but factors like initial PFAS concentration and co-existing substances also matter. It can yield 88–97% PFAS reduction [38]. However, it can generate fine particles, requiring additional measures for containment and disposal. The scale-up application is still in the early stage of development.

### 3.2.3. E-Beam

The use of a high-energy electron beam (E-beam) is another technology employed to remediate PFAS contaminants [39]. A defluorination efficiency of 36% was reported in the presence of oxygen, suggesting that additives or co-existing substances and the dissolved oxygen should be well-controlled [40]. Most likely, PFAS were reduced, rather than oxidized, due to the E-beam's action, which can potentially be harmful to the operators. E-beam irradiation has a limited penetration depth and can also generate toxic by-products.

## 3.3. AOP

Similar to the E-beam approach, AOP employs the high reactivity of radicals for the degradation of organics based on the in-situ generation of radicals such as hydroxyl radicals ( $\bullet\text{OH}$ ) and sulfate radicals ( $\text{SO}_4\bullet^-$ ) [41]. Other radicals that can be generated include superoxide ( $\text{O}_2\bullet^-$ ), carbonate radicals ( $\text{CO}_3\bullet^-$ ), chlorine radicals ( $\text{Cl}\bullet^-$  and  $\text{Cl}_2\bullet^-$ ), etc. [30]. These radicals can react with organic contaminants including PFAS, enabling their degradation and mineralization via redox reactions [41], eventually being converted to carbon dioxide, water, and other inorganics or ions.

The AOP methods are graphically represented in Figure 3, which is based on the activation methods of the radicals, such as ozone ( $\text{O}_3$ )-based, UV-based, catalytic (c-AOP) Fenton reactions, electrochemical (e-AOP) and physical (p-AOP) methods such as ultrasonication, etc. [30]. The above E-beam approach can also be categorized as p-AOP.

Table 1 compares the energy consumption and efficiency of different technologies for PFAS degradation, highlighting the notable advantages of ultrasonication, including its effective degradation of PFAS compounds and minimal by-product formation, compared to other listed technologies.

**Table 1.** Comparison of the energy consumption and highlights of various PFAS degradation technologies.

	Process	Energy Consumption (kWh/m <sup>3</sup> /Order)	Volume (mL)	Time (h)	PFAS	Highlights	Degradation Efficiency	Reference
Non-AOP	E-beam	31–176	10–100		PFOA PFOS	Efficient for concentrated streams Production of reducing species	52–88	[42]
	Electrochemical oxidation	64–98	80	6	PFOA PFOS 6:2FTS	Polarity reversal can reduce energy consumption Polarity reversal effectively mitigates fouling and aging	40–71	[43]
	Ultrasonication	502–1644	500	1.5	GenX PFOA PFOS	No by-products in the samples Effective PFAS degradation	70–90	[44]
AOP	Plasma	23.2–213.4	35–45	1	PFOS PFOA PFNA 8:2FTS	Small conversion to quantifiable PFAS Non-thermal air plasma is promising	>90	[45]
	Photochemical (UV/Sulfite + Iodide)	1.5	600	24	PFCAAs PFSAAs	Enhanced degradation Increased sulfate utilization	>90 >99.7	[46]
	Microwave and iron-activated persulfate (PS)	5714	50	8	PFOA	Synergetic effect with zero-valent iron (ZVI) to degrade PFOA ZVI lowers the activation energy of PS	68	[47]

From the above table, it can be seen that ultrasonication offers rapid and efficient PFAS degradation under some optimized conditions due to its ability to generate high-intensity acoustic cavitation and reactive species. It is worth noting that other technologies might result in the formation of short-chain PFAS compared to the ultrasonication method. However, further research to reduce the costs associated with electrical energy consumption is critical, particularly towards field applications, as discussed below.

#### 4. Ultrasonic Degradation of PFAS

##### 4.1. Degradation Pathway

In ultrasonication, ultrasonic waves propagate through the liquids, generating micro-bubbles and expansion [7]. During expansion, micro-bubbles are formed due to the energy intensity that exceeds the molecular forces of liquid, and collapse during compression [7]. The collapse can generate a high temperature and pressure of approximately 5000 K and 1000 atm, respectively, sufficient to convert water vapor into H<sup>•</sup> + OH<sup>•</sup> radicals (towards the indirect degradation of PFAS) and pyrolyze the fluorinated compounds (direct degradation of PFAS) [7,28,48]. The pathway of PFAS degradation is proposed and represented in Figure 4. The main affecting factors are listed in Table S2 (Supporting Information) and summarized in Figure 5.

Because most PFAS behave as surfactants, they are likely to accumulate at the cavitation bubble–liquid solution interface, with the hydrophilic head oriented toward the bulk liquid and the hydrophobic tail in the micro-bubble gas phase [49]. Also, because PFAS molecules (such as those with a length of ~1 nm) [50] are smaller than the ultrasonic micro-bubbles (ambient radius of 3.5 μm, for example, for a 300 kHz cavity under a bar pressure of 4.6) [51], it is possible for PFAS to accumulate at the bubble surface before cavity collapse [10].



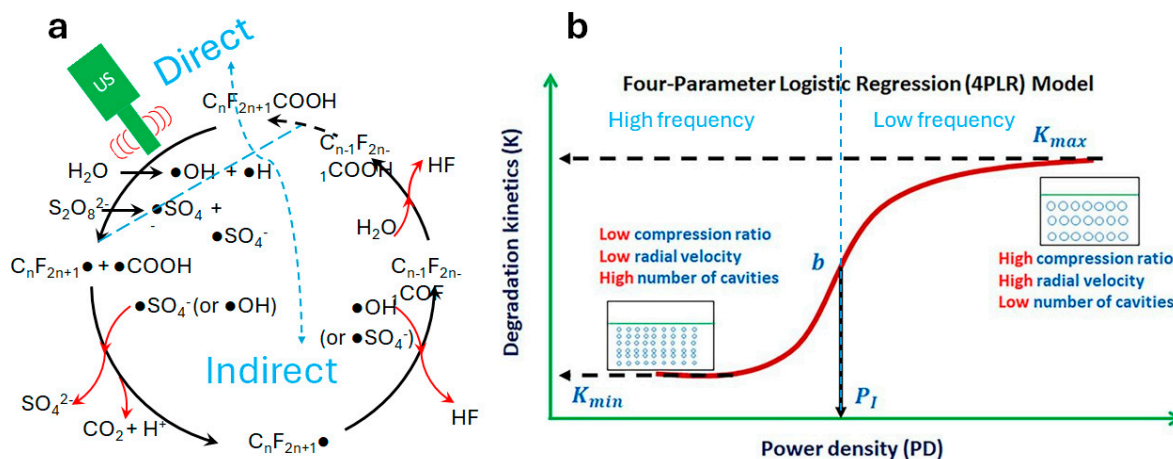


**Figure 4.** Proposed degradation pathway of PFOA, with persulfate ( $S_2O_8^{2-}$ ) used as an oxidant to enhance degradation (a) [6], with permission. Copyright 2020 Elsevier. Relation between power density and cavitation event (b) [52], with permission. Copyright 2021 Elsevier. In (a), the possible oxidants of radicals are suggested, along with the intermediates and products. Each cycle of reaction is initialized by ultrasonication (US) irradiation (as the rate–controlling step), followed by radical oxidation, and ends with the generation of a PFAS intermediate ( $C_{n-1}F_{2n-1}COOH$ , including PFHpA ( $C_6F_{13}COOH$ ), PFHxA ( $C_5F_{11}COOH$ ), PFPeA ( $C_4F_9COOH$ ), and PFBA ( $C_3F_7COOH$ )), with one less  $CF_2$  unit. The initial step for PFOA degradation involves the rapid cleavage of the carboxyl group without releasing  $F^-$ , followed by the pyrolytic degradation of the remaining molecule. In (b), the left side of the figure shows that high frequency typically results in an abundance of cavities with a small radius, low radial velocity, and low compression ratio. Conversely, the right side shows that low frequency produces fewer cavities with a large radius, high radial velocity, and high compression ratio.

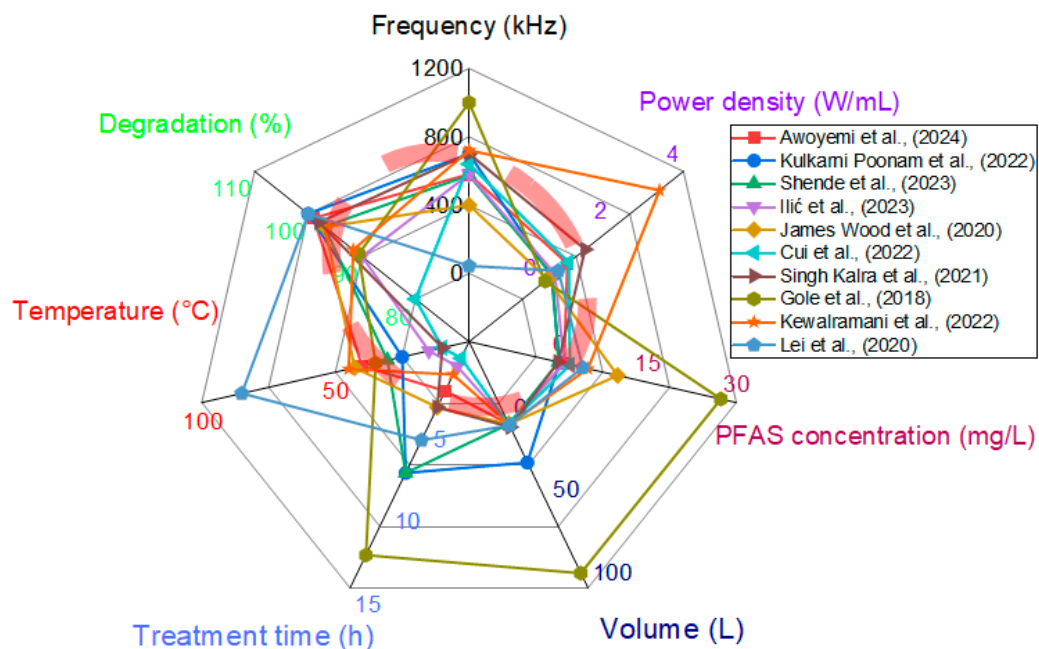


**Figure 5.** Radar chart of recent studies on the ultrasonication of PFAS. The degradation performance is defined as either the removal percentage or the defluorination percentage of PFAS. Power is converted by multiplying power density ( $W/mL$ ) by volume ( $mL$ ). The PFAS concentration is the initial one. The temperature is either controlled using a cooling system or due to Joule heat. The circled area marks the mainly optimized operational parameters. References [6,23–25,44,53–57].

The degradation mechanism of PFAS by AOPs is not clear. It is generally assumed that two steps occur subsequently, as shown in Figure 4a: (i) the direct cleavage of carbon-carbon (C-C) bonds to remove the head functional groups of PFAS and to generate PFAS C-F backbone radicals that enable the subsequent indirect steps, and (ii) the generated PFAS radicals are attacked by the highly AOP radical, such as  $\bullet\text{OH}$  and  $\text{SO}_4^{\bullet-}$ , to gradually destroy the C-F bonds towards full mineralization. The first step is usually the rate-control step and needs a high energy input to initiate the PFAS degradation process. In Figure 4a, the initiation is activated by ultrasonication. The ultrasonic process also generates radicals for the subsequent reaction to gradually shorten the carbon chain of the C-F backbone towards full mineralization.

Figure 4b demonstrates that high frequencies generate a higher number of cavities compared to low frequencies, enhancing PFAS degradation by creating favorable conditions for redox reactions and promoting mass transportation. In an ultrasonication system, the frequency determines the size and collapse intensity of micro-bubbles, influencing radical production [58]. In brief, low frequencies (20–100 kHz) produce large bubbles, while mid-frequencies (100–1000 kHz) result in a higher cavity population due to rapid diffusion and quick bubble collapse [9,10]. High frequencies (above 1000 kHz) reduce  $\text{OH}\bullet$  radical populations due to faster compression cycles and smaller bubbles [59,60].

#### 4.2. Affecting Factors

Figure 5 presents the radar chart of recent studies on the ultrasonication of PFAS. Each axis represents one parameter: frequency (kHz), volume (L), power density (W/mL), PFAS concentration (mg/L), treatment time (h), temperature ( $^{\circ}\text{C}$ ), and degradation (%). The data from each study form a unique polygon, allowing for the easy comparison of how the different studies align or differ in terms of these parameters.

The radar chart analysis of ultrasonication parameters for PFAS degradation reveals some important insights as follows. (i) The standard deviation values (estimated by calculating the specific parameters from all cited references) reveal the extent of variation for each parameter, such as power density (0.9), treatment time (3.7), degradation percentage (6.3), PFAS concentration (8.4), temperature (22.2), volume (28.7), and frequency (246.6). (ii) In Figure 5, power density shows the least deviation, indicating that this parameter is relatively consistent across different studies or that high-power density is always needed. (iii) In contrast, treatment time, degradation efficiency, and PFAS concentration exhibit moderate variability, suggesting that while effective degradation can be achieved, optimization is needed. (iv) Parameters such as temperature and volume show high deviation, indicative of the challenge towards scale-up application without new tests, such as pilot or trial projects. (v) Notably, frequency exhibits the highest deviation, indicating substantial variation in different studies, either due to the variation in the instrument or owing to the fabrication approach. Overall, the chart underscores the consistency of certain parameters while pointing out (via a red circle) areas requiring more investigation for improved ultrasonication efficacy (not just degradation efficiency but also energy consumption efficiency), the lowest PFAS concentration that can be reached, the treatment volume and duration, the costs, etc. By identifying optimal ranges and interactions among these variables, it is possible to maximize degradation efficiency through the development of robust and scalable protocols.

##### 4.2.1. Frequency

Comparing the PFAS degradation rates ( $3.4 \times 10^{-4}$ – $5.7 \times 10^{-4} \text{ min}^{-1}$ ) at low frequencies (such as 28 kHz and 40 kHz) [61,62], the rates ( $6.8 \times 10^{-3}$ – $0.032 \text{ min}^{-1}$ ) at mid frequencies (200 kHz and 358 kHz) show more efficiency in degrading PFAS [55,63]. GenX, a different PFAS, degrades faster than PFOA and PFOS at a mid-high frequency (580 kHz) [44], suggesting the effect of the PFAS type, as discussed below.



As shown in Table S2 (Supporting Information), several mid-frequency tests result in a more effective PFAS degradation. For example, degradation percentages of 97% and 94% were observed for PFOS at 400 and 500 kHz, respectively, compared to 91% observed at 1000 kHz [55]. Similar results were observed in [44,64], where a higher degradation of PFOS and PFOA was reported at the mid-frequency zone than at the high-frequency zone. The reason for higher degradation at mid frequencies is because the number of active sites on the interface of the cavitation micro-bubble used for adsorption increases at such mid-frequencies. This results in greater mass transportation from the bulk solution to the cavitation bubble interface, leading to more extensive decomposition by interfacial pyrolysis [9]. This step is usually the rate-control one, as discussed above.

#### 4.2.2. Power Density

Figure 4b shows that with increasing power density, the compression ratio and radial velocity of micro-bubbles increase, leading to more intense pressure differences and more effective cavitation events. Higher acoustic power, which represents the energy emitted by a power source, increases the number of collapse cavities and  $\text{OH}^\bullet$  production [58,65]. For a constant solution volume, increased power also enhances intensity and mass transfer rates due to turbulence from bubble collapse [66]. As shown in Table S2 (Supporting Information), various power densities were used for PFAS remediation. Power density (up to 1 W/mL) was mostly used for PFAS degradation, except for PFAS degradation in soil slurry media, where a power density as high as 3.33 W/mL was used. In the latter case, the high energy requirement is associated with the strong hydrophobic interaction between PFAS and soil organic matter [67].

#### 4.2.3. Structural Effect of PFAS (Terminal Head) and pH

In terms of the functional headgroup, PFCAs degrade faster than PFASs of the same carbon chain length due to the larger size and greater shielding effect of the sulfonic group ( $-\text{SO}_3\text{H}$ ) compared to the carboxyl group ( $-\text{COOH}$ ) [1,10]. This was demonstrated by Vecitis and colleagues, who reported a faster degradation rate for PFOA ( $0.041 \text{ min}^{-1}$ ) than PFOS ( $0.027 \text{ min}^{-1}$ ) [68]. However, in samples containing both PFOS and PFOA at concentrations beyond saturation, PFOS degrades faster [68,69]. More research is needed to confirm the mechanism behind it, as indicated in Figure 4a.

Solution pH significantly impacts PFAS degradation, with an optimal pH of around 4.0 for PFOS [56] and 4.3 for PFOA [70]. Low pH reduces the recombination of  $\text{OH}^\bullet$  radicals and deprotonation of PFAS terminal groups [56] for example, facilitating a better accumulation at the water–bubble interface, thus enhancing degradation [71]. These findings underscore the complex interplay of chemical properties and environmental conditions in the PFAS degradation.

#### 4.2.4. PFAS Concentration

The degradation of PFAS is believed to occur at the bubble–water interface due to their hydrophobic nature [48]. The critical micelle concentration (CMC) indicates the effect of the concentration [72]. However, the CMC is usually in mM [73], much higher than the PFAS in the environmental samples ( $\mu\text{M}$  or less), suggesting that micelle formation is unlikely without high concentrations of co-existing surfactants.

As the water–bubble interface becomes saturated, there is a rate transition from the pseudo-first order to the zero order. For example, in [72], the ultrasonication kinetics of PFOX ( $X = A$  for PFOA, or  $S$  for PFOS, for example) transitioned from the pseudo-first order at low initial concentrations ( $<20 \mu\text{M}$ ) to zero-order kinetics at high concentrations ( $>40 \mu\text{M}$ ). Similar results were observed in [69], where PFOX followed the pseudo-first order at lower concentrations ( $<2.34 \mu\text{M}$  and  $<400 \text{ pM}$ , respectively) and the zero order at higher concentrations ( $>23.60 \mu\text{M}$  and  $>400 \text{ pM}$ , respectively). The detailed mechanism is still not clear but might be related to the accumulation at the water–bubble surface.

#### 4.2.5. Solution Volume and Treatment Time

For a constant power input, increasing the solution volume can reduce the power density, thereby resulting in a decline in degradation performance [52]. It was reported that a decrease in the volume of solution from 500 mL to 200 mL at 575 kHz, 860 kHz, and 1140 kHz increases the degradation rate by 2.7 times, 3.8 times, 1.8 times for PFOS and 3.1 times, 4.5 times, 3.9 times for PFOA, respectively. The effect of liquid height on ultrasonication efficiency shows that the sonoluminescence becomes vertically elongated and narrows as the liquid height increases [74]. In the meantime, the location of the transducer (on the top or the bottom and via a probe or transducer) and reactor geometry determine the direction of propagation of the ultrasonic power [75]. For scale-up applications, the configuration of setup should be balanced among the degradation performance, fabrication and cost.

On the other hand, treatment duration or time is inversely correlated to PFAS degradation efficiency. In an ultrasonication system, prolonged duration usually increases the PFOA degradation percentage, regardless of whether the process follows first-order or zero-order kinetics [76]. However, from an economic point of view, to reduce energy costs, short treatment time should be employed and the ultrasonic approach should be combined with other processes like electrochemistry, as discussed later [77].

#### 4.2.6. Additives

The low degradation rate of PFAS at low frequencies (20–100 kHz) can be enhanced by the addition of additives such as oxidant [6,71,76]. The use of persulfate (such as  $K_2S_2O_8$ ), which is activated as a radical of  $SO_4^{\bullet-}$ , can enhance the degradation of PFOA [6]. Similar enhancement was reported with permanganate, where the degradation rate constant of PFOA is higher in the presence of permanganate than in its absence [76]. Iodate radical ( $IO_3^{\bullet-}$ ) and  $CO_3^{\bullet-}$  have also been introduced to ultrasonication to enhance PFOA degradation. Periodate was used to activate  $IO_3^{\bullet-}$  [71], and sodium bicarbonate was used to activate  $CO_3^{\bullet-}$  [78]. Beyond the oxidant additive that can be helpful for PFAS degradation, some additives are present as co-constituents with PFAS and compete with PFAS degradation, thereby interfering with the degradation process.

#### 4.2.7. Co-Existent Inorganic Constituents and Co-Existent Contaminants

In the application of sonication, inorganic substances might have some effects [48]. For example, a study showed that the PFAS ultrasonic degradation rates in groundwater are 20.5–29.7% lower than those in Milli-Q water [79]. The presence of inorganic anions shows Hofmeister effects on the ultrasonic degradation of PFOX, with  $ClO_4^- > NO_3^- > Cl^- > HCO_3^- > SO_4^{2-}$ , with  $ClO_4^-$ ,  $NO_3^-$ , and  $Cl^-$ , enhancing the rates, while  $HCO_3^-$  and  $SO_4^{2-}$  showing negative effects. Regarding the effects of cations,  $Na^+$ ,  $Ca^{2+}$ , and  $Mg^{2+}$  were negligible in PFOA degradation [79]. However,  $Cu^{2+}$ ,  $Fe^{2+}$ , and  $Fe^{3+}$  ions could hinder PFOA degradation in the permanganate-ultrasonication system [76]. The reason is not clear yet.

There is potential competition at the bubble–water interface by co-existent organic contaminants. Also, the evaporation of volatile organic compounds (VOCs) consumes the destructive ultrasonic energy through the endothermic process [80]. However, the presence of organic compounds like carbon tetrachloride ( $CCl_4$ ) in the water matrix is believed to improve the ultrasonic degradation of organic pollutants [81], including PFAS. This is due to the formation of hypochlorous acid (HOCl), chlorine-type radicals ( $Cl^{\bullet}$  and  $\bullet CCl_3$ ), and chlorine ( $Cl_2$ ) from the sonication of  $CCl_4$ , in addition to  $HO^{\bullet}$  radicals. More research is needed on this topic.

#### 4.2.8. Dissolved Gas

In the presence of gas, the production of  $OH^{\bullet}$  in water occurs in the following order:  $Kr > Ar > He > O_2$  [82]. That is, the ultrasonic degradation of PFAS under Ar shows faster

degradation rates than under air [49,62,76]. However, on an industrial scale, the cost associated with the use of Ar should be considered.

#### 4.2.9. Other Factors: Configuration, Reactor Geometry, and Co-Occurring PFAS

The impact of reactor geometry on PFAS destruction was studied in [83], which showed that placing the transducer along the bottom and side wall of the reactor had no significant impact on ultrasonication activity. Moreover, using dual transducers (side and bottom) did not produce a synergistic effect but instead reduced ultrasonication activity due to disturbances caused by the interaction of ultrasonic fields from both transducers.

The impact of co-occurring PFAS in solution during ultrasonication treatment was studied on six PFAS compounds (PFCAs (C4, C6, and C8) and PFSA (C4, C6, and C8)) in [84]. The study showed that long-chain PFAS decreased at a faster rate than short-chain PFAS, due to the lower hydrophobicity of short-chain PFAS. Similar results were reported in [63,68,83]. Additionally, PFCAs degrade faster than PFSA of the same chain length, as stated earlier [8,10,68]. Overall, the results suggest that the hydrophilic functional group contributes to the rate of PFAS degradation [84]. Also, Shende and colleagues experimented on the degradation of 13 PFAS mixtures (PFCAs (C4–C14) and PFSA (C6–C8)) [54]. The authors reported a higher rate of breakdown of PFAS mixtures than that of individual PFAS. The authors compared the G-value (the efficiency of chemical reactions induced by ultrasonic energy) for the degradation of the 13 PFAS mixtures ( $14.23 \times 10^{13}$  molecules/kJ) to the G-value for PFOA degradation by the electrochemical method ( $7.07 \times 10^{13}$  molecules/kJ) and plasma ( $1312 \times 10^{13}$  molecules/kJ). They suggested that the ultrasonic degradation of PFAS mixtures is a variable alternative, although it is less energy-efficient compared to plasma method.

#### 4.3. Ultrasonication Combined with Other Techniques as the Hybrid Method

Recent research has explored the use of AOPs in conjunction with ultrasonication as hybrid techniques to further enhance degradation efficiency. In Figure 3, ultrasonication can be combined with other AOPs, as shown in Figure 6, including electrochemistry [77], UV [85], photocatalyst [61], and others. Hybrid approaches in the degradation of PFAS are important because they leverage the strengths of multiple techniques to achieve more efficient and effective PFAS breakdown. Some degradation techniques, while powerful, have limitations in terms of efficiency and completeness when used alone.

Ultrasonication is compatible with other AOP approaches because it does not require chemicals. As a p-AOP, it degrades PFAS by cavity-generating micro-bubbles that can be easily combined with other chemical-based AOPs, such as ozone-based, UV-based, c-AOP, and e-AOP which use electrochemistry reactions. Ultrasonication is commonly used in labs for cleaning and dispersion purposes; so, it is generally available in most labs, particularly for low-frequency (e.g., 20–40 kHz) applications. Cleaning and dispersion, realized by the sound wave-based micro-bubble compression/collapse, can also benefit other AOPs, such as by accelerating mass transportation (to replace stirring in most cases), homogenizing the solution, targeting and cleaning the electrode surface (to avoid fouling and poisoning), assisting with the activation of catalysis (such as oxidants to radicals), etc. Intrinsic PFAS degradation by ultrasonication can be thus enhanced or be used to enhance the combined techniques (to be expressed by an enhancement factor, as discussed below). Furthermore, the combination can also inherit the advantages of only using AOP toward a synergistic effect to increase degradation efficiency, decrease energy consumption, and shorten the treatment time. These can all help with scale-up applications towards site remediation.

Table S3 (Supporting Information) shows the ultrasonication hybrid, which is summarized in Figure 6. The comparison of the degradation efficiency of the hybrid method to the efficiency of ultrasonication or other technologies is represented in Figure 6a. Similar to Figure 5, the data from each study form a unique shape (triangle) (Figure 6b), allowing for the easy comparison of how the different hybrid studies align or differ.

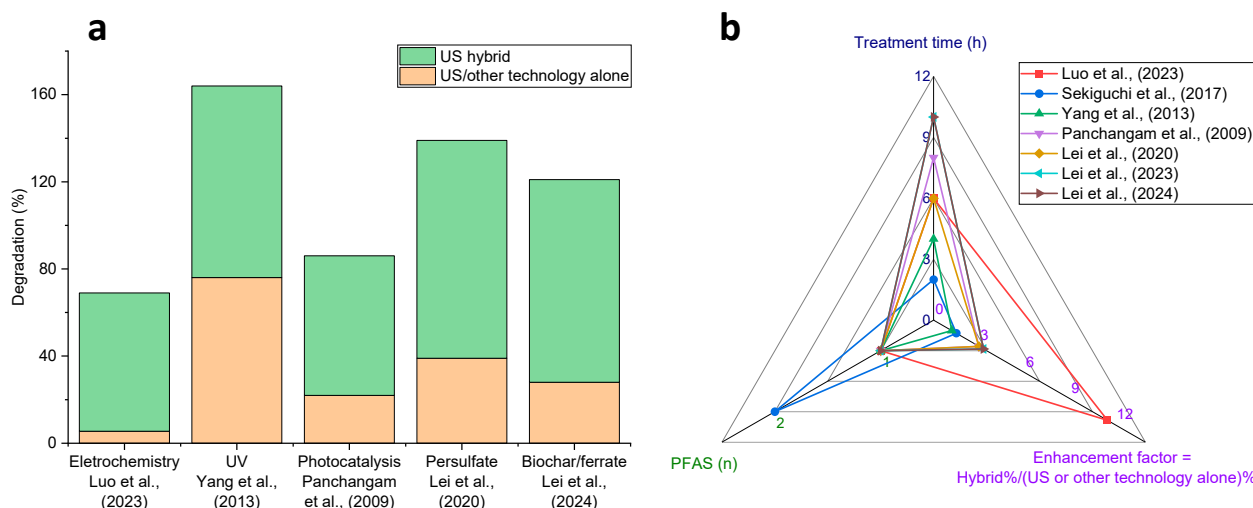


**Figure 6.** Degradation efficiency of different ultrasonication hybrid methods (a) and radar chart of ultrasonication hybrid methods for PFAS degradation (b). Ultrasonication with electrochemistry [77], UV [85,86], photocatalysis [61], persulfate [6,87], and biochar/ferrate [88]. The enhancement factor specifies how many times PFAS were degraded compared to US (ultrasonication) or other technologies, which has an enhancement factor of 1. The number of PFAS includes different types, such as PFOA and PFOS. References [6,61,77,85–88].

#### 4.3.1. Ultrasonication/Electrochemistry

The hybrid system of electrochemistry and ultrasonication studied in [77] shows that the synergistic effect between the Magnéli-phase  $Ti_4O_7$ -based electrochemistry process and the ultrasonication system operated at 130 kHz, 100 W, and 0.83 W/mL. For 6 h degradation of 50  $\mu$ M PFOA can improve the defluorination of PFOA. They reported that the hybrid yielded a defluorination of 63.5%, which is higher than the sum (43% and 5.5%) achieved by electrochemistry and ultrasonication alone, respectively. The synergistic effect was attributed to improved mass transfer, activated electrode surface, and enhanced production of radicals, as proposed above. The robustness of the hybrid was extended to three real samples of AFFF.

#### 4.3.2. Ultrasonication/UV

A hybrid system of ultraviolet (UV, @185 nm)-assisted ultrasonication (600 kHz) was conducted in [85] to defluorinate PFOS under an air atmosphere. They reported a synergistic defluorination of 88% of PFOS (10 mg/L), which is 12% higher than that achieved using only an ultrasonication system operated at 100 W and 0.2 W/cm<sup>2</sup> for 4 h. The authors also observed that the UV-assisted ultrasonication system generated lower intermediates than the ultrasonic system alone, suggesting that the hybrid system can degrade both the PFOS and its intermediates more effectively.

Panchangam and colleagues combined an ultrasonication system (40 kHz) with a commercial UV system (254 nm) [61]. The degradation efficiency of the PFOA of the hybrid was reported at 64%, higher than when the hybrid system was run in sequential mode and photocatalysis (25% and 22%, respectively). More hybrid research can be expected in the coming years.

#### 4.3.3. Ultrasonication/Oxidant

The synergistic effect of ultrasonication and persulfate has been considered. This hybrid system promotes the activation of  $SO_4^{\bullet-}$ ,  $E^\circ = 2.6$  V [6], which can enhance PFAS degradation through radical attack of indirection degradation. The addition of persulfate to ultrasonication thus increases the degradation of PFAS. After a 6 h treatment, the defluorination percentages of PFOA by persulfate (0.77%) and ultrasonication (14.6% at 20 kHz

and 20% at 43 kHz) alone increased to 33.2% and 38.3%, respectively, compared to the hybrid [6]. Later, Lei and colleagues reported a ~100% defluorination percentage when both frequencies were used with persulfate-coupled ultrasonication [87]. Furthermore, surfactants including sodium dodecyl sulfate (SDS), cetyltrimethylammonium bromide (CTAB), and Triton X-100 were used to enhance the degradation as well. Although the defluorination percentage is low, the study showed that an indirect persulfate/ultrasonication system at low frequency is a potential ultrasonication hybrid, which can be explored to further enhance the defluorination of PFAS.

#### 4.3.4. Multiple Ultrasonication

A triple ultrasonication hybrid was formed in a study, combining rice straw biochar-assisted ultrasonication with ferrate (Fe VI) [88]. This combination achieved a higher defluorination (93%) after 10 h of treatment at 43 kHz and 0.25 W/mL, compared to other hybrid methods tested (ultrasonication/biochar and ultrasonication/Fe VI hybrids), which achieved 28% and 49% defluorination, respectively. The hybrid induces an increase in the specific surface area of biochar, enhancing its capacity for PFOA adsorption, and promotes the generation of  $\bullet\text{OH}$  and intermediate iron species (Fe (V) and Fe (IV)), enhancing the degradation of PFOA. The reusability of the biochar was tested, and defluorination was reduced by ~14% after five cycles. Overall, the ultrasonication/biochar/Fe (VI) hybrid system enhances PFOA defluorination. However, additional technology will be required to destroy the PFOA adsorbed on the spent biochar.

#### 4.3.5. Ultrasonication/Foam Fractionation

Foam fractionation/ultrasonication hybrid is a potential method for PFAS destruction [23]. The authors ultrasonicated foam fractionate, that is, the concentrated and separated PFAS-containing foam, and observed a reduction of ~97% in the total PFAS levels after 3 h of treatment at 0.75 W/mL and 580 kHz. These findings underscore the feasibility and effectiveness of coupling ultrasonication with the currently applied PFAS remediation plants. Most of the current plants only remove PFAS from the environment and yield the concentrated PFAS, as said. The concentrated PFAS can be easily degraded, for example, by ultrasonication. This two-step approach of hybrid holds significant promise for addressing PFAS contamination in various environmental settings, with potential for scale-up or site applications.

## 5. Prospects and Future Directions

As PFAS remediation continues to evolve, there are several prospects and directions for future research on ultrasonication technology, as proposed below.

- (i) The refinement and optimization of ultrasonication equipment and techniques to enhance its efficiency and effectiveness for scale-up or on-site applications.
- (ii) The development of cost-effective and scalable ultrasonication solutions for PFAS remediation in various matrices and contamination scenarios. Currently, its widespread implementation may be hindered by a liquid-based matrix only.
- (iii) The integration of ultrasonication with other remediation methods and technologies to form hybrid systems. However, the complexity of the hybrid system and the extra input of energy should be considered.
- (iv) The challenges and limitations associated with ultrasonication-based PFAS degradation, including a better understanding of PFAS degradation mechanisms, the optimization of operating parameters, and the assessment of potential by-products towards mass balance. Collaborative interdisciplinary research involving experts from chemistry, engineering, environmental science, and toxicology will be essential in advancing our knowledge and capabilities in this field.
- (v) Addressing regulatory and safety concerns regarding field applications of ultrasonication technology for PFAS degradation will be paramount. Compliance with environmental regulations and safety standards is crucial to ensure the responsible use of



ultrasonic treatment methods. This includes the careful consideration of the generation of by-products, potential impacts on surrounding ecosystems, and the effective management of treated effluents.

**Supplementary Materials:** The following supporting information can be downloaded at: <https://www.mdpi.com/article/10.3390/environments11090187/s1>, Table S1. List of abbreviations and acronyms used in this work; Table S2: Summary of recent studies on ultrasonic degradation of PFAS; Table S3: Ultrasonication hybrid for PFAS degradation. References [6,23–25,44,56,59,60,65,75,83–85,87–92] were cited in the Supplementary Materials.

**Author Contributions:** Conceptualization, C.F.; Methodology, O.S.A. and C.F.; Formal analysis, O.S.A.; Investigation, O.S.A.; Data curation, O.S.A.; Writing—original draft preparation, O.S.A.; Writing—review and editing, R.N. and C.F.; Supervision, R.N. and C.F.; Project administration, R.N. and C.F.; Funding acquisition, R.N. and C.F. All authors have read and agreed to the published version of the manuscript.

**Funding:** The authors acknowledge the funding by the Australian Research Council (SR180200015).

**Acknowledgments:** The authors acknowledge the support from the CRC for Contamination Assessment and Remediation of the Environment (CRC CARE) and the Global Centre for Environmental Remediation (GCER) at the University of Newcastle, Australia.

**Conflicts of Interest:** The authors declare that they have no known competing financial interests or personal relationships that could have appeared to have an impact on the work reported in this paper.

## References

1. Fang, C.; Megharaj, M.; Naidu, R. Electrochemical Advanced Oxidation Processes (EAOP) to degrade per- and polyfluoroalkyl substances (PFASs). *J. Adv. Oxid. Technol.* **2017**, *20*, 20170014. [[CrossRef](#)]
2. Glüge, J.; Scheringer, M.; Cousins, I.T.; DeWitt, J.C.; Goldenman, G.; Herzke, D.; Lohmann, R.; Ng, C.A.; Trier, X.; Wang, Z. An overview of the uses of per- and polyfluoroalkyl substances (PFAS). *Environ. Sci. Process. Impacts* **2020**, *22*, 2345–2373. [[CrossRef](#)]
3. Morin-Crini, N.; Lichtfouse, E.; Liu, G.R.; Balaram, V.; Ribeiro, A.R.L.; Lu, Z.J.; Stock, F.; Carmona, E.; Teixeira, M.R.; Picos-Corrales, L.A.; et al. Worldwide cases of water pollution by emerging contaminants: A review. *Environ. Chem. Lett.* **2022**, *20*, 2311–2338. [[CrossRef](#)]
4. Yang, L.; He, L.; Xue, J.; Ma, Y.; Xie, Z.; Wu, L.; Huang, M.; Zhang, Z. Persulfate-based degradation of perfluorooctanoic acid (PFOA) and perfluorooctane sulfonate (PFOS) in aqueous solution: Review on influences, mechanisms and prospective. *J. Hazard. Mater.* **2020**, *393*, 122405. [[CrossRef](#)] [[PubMed](#)]
5. Meegoda, J.N.; Kewalramani, J.A.; Li, B.; Marsh, R.W. A Review of the Applications, Environmental Release, and Remediation Technologies of Per- and Polyfluoroalkyl Substances. *Int. J. Environ. Res. Public Health* **2020**, *17*, 8117. [[CrossRef](#)] [[PubMed](#)]
6. Lei, Y.-J.; Tian, Y.; Sobhani, Z.; Naidu, R.; Fang, C. Synergistic degradation of PFAS in water and soil by dual-frequency ultrasonic activated persulfate. *Chem. Eng. J.* **2020**, *388*, 124215. [[CrossRef](#)]
7. Hoffmann, M.R.; Hua, I.; Höchemer, R. Application of ultrasonic irradiation for the degradation of chemical contaminants in water. *Ultrason. Sonochem.* **1996**, *3*, S163–S172. [[CrossRef](#)]
8. Fernandez, N.A.; Rodriguez-Freire, L.; Keswani, M.; Sierra-Alvarez, R. Effect of chemical structure on the sonochemical degradation of perfluoroalkyl and polyfluoroalkyl substances (PFASs). *Environ. Sci. Water Res. Technol.* **2016**, *2*, 975–983. [[CrossRef](#)]
9. Cao, H.; Zhang, W.; Wang, C.; Liang, Y. Sonochemical degradation of poly- and perfluoroalkyl substances—A review. *Ultrason. Sonochem.* **2020**, *69*, 105245. [[CrossRef](#)]
10. Sidnell, T.; Wood, R.J.; Hurst, J.; Lee, J.; Bussemaker, M.J. Sonolysis of per- and poly fluoroalkyl substances (PFAS): A meta-analysis. *Ultrason. Sonochem.* **2022**, *87*, 105944. [[CrossRef](#)]
11. Al Amin, M.; Luo, Y.; Shi, F.; Yu, L.; Liu, Y.; Nolan, A.; Awoyemi, O.S.; Megharaj, M.; Naidu, R.; Fang, C. A modified TOP assay to detect per- and polyfluoroalkyl substances in aqueous film-forming foams (AFFF) and soil. *Front. Chem.* **2023**, *11*, 1141182. [[CrossRef](#)] [[PubMed](#)]
12. Wiredchemist. Common Bond Energies (D) and Bond Lengths (r). 2023. Available online: [https://www.wiredchemist.com/chemistry/data/bond\\_energies\\_lengths.html](https://www.wiredchemist.com/chemistry/data/bond_energies_lengths.html) (accessed on 25 May 2023).
13. ITRC PFAS Team. PFAS—Per- and Polyfluoroalkyl Substances. Available online: <https://pfas-1.itrcweb.org/> (accessed on 1 December 2023).
14. Hartz, W.F.; Björnsdotter, M.K.; Yeung, L.W.Y.; Hodson, A.; Thomas, E.R.; Humby, J.D.; Day, C.; Jogsten, I.E.; Kärrman, A.; Kallenborn, R. Levels and distribution profiles of Per- and Polyfluoroalkyl Substances (PFAS) in a high Arctic Svalbard ice core. *Sci. Total Environ.* **2023**, *871*, 161830. [[CrossRef](#)]

15. Wang, X.; Halsall, C.; Codling, G.; Xie, Z.; Xu, B.; Zhao, Z.; Xue, Y.; Ebinghaus, R.; Jones, K.C. Accumulation of Perfluoroalkyl Compounds in Tibetan Mountain Snow: Temporal Patterns from 1980 to 2010. *Environ. Sci. Technol.* **2014**, *48*, 173–181. [[CrossRef](#)]
16. Taylor, S.; Terkildsen, M.; Stevenson, G.; de Araujo, J.; Yu, C.; Yates, A.; McIntosh, R.R.; Gray, R. Per and polyfluoroalkyl substances (PFAS) at high concentrations in neonatal Australian pinnipeds. *Sci. Total Environ.* **2021**, *786*, 147446. [[CrossRef](#)] [[PubMed](#)]
17. Harris, K.J.; Munoz, G.; Woo, V.; Sauv e, S.; Rand, A.A. Targeted and Suspect Screening of Per- and Polyfluoroalkyl Substances in Cosmetics and Personal Care Products. *Environ. Sci. Technol.* **2022**, *56*, 14594–14604. [[CrossRef](#)] [[PubMed](#)]
18. Place, B.J.; Field, J.A. Identification of Novel Fluorochemicals in Aqueous Film-Forming Foams Used by the US Military. *Environ. Sci. Technol.* **2012**, *46*, 7120–7127. [[CrossRef](#)]
19. Kurwadkar, S.; Dane, J.; Kanel, S.R.; Nadagouda, M.N.; Cawdrey, R.W.; Ambade, B.; Struckhoff, G.C.; Wilkin, R. Per- and polyfluoroalkyl substances in water and wastewater: A critical review of their global occurrence and distribution. *Sci. Total Environ.* **2022**, *809*, 151003. [[CrossRef](#)]
20. USEPA. EPA Proposes Designating Certain PFAS Chemicals as Hazardous Substances Under Superfund to Protect People’s Health. 2022. Available online: <https://www.epa.gov/newsreleases/epa-proposes-designating-certain-pfas-chemicals-hazardous-substances-under-superfund> (accessed on 15 December 2022).
21. USEPA. Questions and Answers: Drinking Water Health Advisories for PFOA, PFOS, GenX Chemicals and PFBS. 2023. Available online: <https://www.epa.gov/sdwa/questions-and-answers-drinking-water-health-advisories-pfoa-pfos-genx-chemicals-and-pfbs> (accessed on 27 June 2023).
22. Ertekin, A.; Kausch, C.M.; Kim, Y.; Thomas, R.R. Synthesis, Characterization, Adsorption, and Interfacial Rheological Properties of Four-Arm Anionic Fluorosurfactants. *Langmuir* **2008**, *24*, 2412–2420. [[CrossRef](#)]
23. Awoyemi, O.S.; Luo, Y.; Niu, J.; Naidu, R.; Fang, C. Ultrasonic degradation of per-and polyfluoroalkyl substances (PFAS), aqueous film-forming foam (AFFF) and foam fractionate (FF). *Chemosphere* **2024**, *360*, 142420. [[CrossRef](#)]
24. Singh Kalra, S.; Cranmer, B.; Dooley, G.; Hanson, A.J.; Maraviov, S.; Mohanty, S.K.; Blotevogel, J.; Mahendra, S. Sonolytic destruction of Per- and polyfluoroalkyl substances in groundwater, aqueous Film-Forming Foams, and investigation derived waste. *Chem. Eng. J.* **2021**, *425*, 131778. [[CrossRef](#)]
25. Cui, D.; Abdullah, A.M.; Peller, J.R.; Mezyk, S.P.; Mebel, A.; O’Shea, K. Effectiveness of Photocatalysis, Radiolysis, and Ultrasonic Irradiation in the Remediation of GenX: Computational Study of the Ultrasonically Induced Mineralization. *J. Environ. Eng.* **2022**, *148*, 04022073. [[CrossRef](#)]
26. Franke, V.; Sch afers, M.D.; Joos Lindberg, J.; Ahrens, L. Removal of per- and polyfluoroalkyl substances (PFASs) from tap water using heterogeneously catalyzed ozonation. *Environ. Sci. Water Res. Technol.* **2019**, *5*, 1887–1896. [[CrossRef](#)]
27. Leung, S.C.E.; Shukla, P.; Chen, D.; Eftekhari, E.; An, H.; Zare, F.; Ghasemi, N.; Zhang, D.; Nguyen, N.-T.; Li, Q. Emerging technologies for PFOS/PFOA degradation and removal: A review. *Sci. Total Environ.* **2022**, *827*, 153669. [[CrossRef](#)] [[PubMed](#)]
28. Meegoda, J.N.; Bezerra de Souza, B.; Casarini, M.M.; Kewalramani, J.A. A review of PFAS destruction technologies. *Int. J. Environ. Res. Public Health* **2022**, *19*, 16397. [[CrossRef](#)] [[PubMed](#)]
29. Nzeribe, B.N.; Crimi, M.; Mededovic Thagard, S.; Holsen, T.M. Physico-Chemical Processes for the Treatment of Per- And Polyfluoroalkyl Substances (PFAS): A review. *Crit. Rev. Environ. Sci. Technol.* **2019**, *49*, 866–915. [[CrossRef](#)]
30. Miklos, D.B.; Remy, C.; Jekel, M.; Linden, K.G.; Drewes, J.E.; H ubner, U. Evaluation of advanced oxidation processes for water and wastewater treatment—A critical review. *Water Res.* **2018**, *139*, 118–131. [[CrossRef](#)]
31. Yamada, T.; Taylor, P.H.; Buck, R.C.; Kaiser, M.A.; Giraud, R.J. Thermal degradation of fluorotelomer treated articles and related materials. *Chemosphere* **2005**, *61*, 974–984. [[CrossRef](#)]
32. Bulm au, C.; M arculescu, C.; Lu, S.; Qi, Z. Analysis of thermal processing applied to contaminated soil for organic pollutants removal. *J. Geochem. Explor.* **2014**, *147*, 298–305. [[CrossRef](#)]
33. Sorengard, M.; Lindh, A.S.; Ahrens, L.; DeWitt, J.C. Thermal desorption as a high removal remediation technique for soils contaminated with per- and polyfluoroalkyl substances (PFASs). *PLoS ONE* **2020**, *15*, e0234476. [[CrossRef](#)]
34. Trang, B.; Li, Y.; Xue, X.-S.; Ateia, M.; Houk, K.N.; Dichtel, W.R. Low-temperature mineralization of perfluorocarboxylic acids. *Sci. Am. Assoc. Adv. Sci.* **2022**, *377*, 839–845. [[CrossRef](#)]
35. Al Amin, M.; Luo, Y.; Nolan, A.; Mallavarapu, M.; Naidu, R.; Fang, C. Thermal kinetics of PFAS and precursors in soil: Experiment and surface simulation in temperature-time plane. *Chemosphere* **2023**, *318*, 138012. [[CrossRef](#)] [[PubMed](#)]
36. Solares-Briones, M.; Coyote-Dotor, G.; P aez-Franco, J.C.; Zerme no-Ortega, M.R.; de la O Contreras, C.M.; Canseco-Gonz alez, D.; Avila-Sorrosa, A.; Morales-Morales, D.; Germ an-Acacio, J.M. Mechanochemistry: A Green Approach in the Preparation of Pharmaceutical Cocrystals. *Pharmaceutics* **2021**, *13*, 790. [[CrossRef](#)] [[PubMed](#)]
37. Wang, N.; Lv, H.; Zhou, Y.; Zhu, L.; Hu, Y.; Majima, T.; Tang, H. Complete Defluorination and Mineralization of Perfluorooctanoic Acid by a Mechanochemical Method Using Alumina and Persulfate. *Environ. Sci. Technol.* **2019**, *53*, 8302–8313. [[CrossRef](#)]
38. Turner, L.P.; Kueper, B.H.; Jaansalu, K.M.; Patch, D.J.; Battye, N.; El-Sharnouby, O.; Mumford, K.G.; Weber, K.P. Mechanochemical remediation of perfluorooctanesulfonic acid (PFOS) and perfluorooctanoic acid (PFOA) amended sand and aqueous film-forming foam (AFFF) impacted soil by planetary ball milling. *Sci. Total Environ.* **2021**, *765*, 142722. [[CrossRef](#)] [[PubMed](#)]

39. Wang, L.; Batchelor, B.; Pillai, S.D.; Botlaguduru, V.S.V. Electron beam treatment for potable water reuse: Removal of bromate and perfluorooctanoic acid. *Chem. Eng. J.* **2016**, *302*, 58–68. [[CrossRef](#)]
40. Lassalle, J.; Gao, R.; Rodi, R.; Kowald, C.; Feng, M.; Sharma, V.K.; Hoelen, T.; Bireta, P.; Houtz, E.F.; Staack, D.; et al. Degradation of PFOS and PFOA in soil and groundwater samples by high dose Electron Beam Technology. *Radiat. Phys. Chem.* **2021**, *189*, 109705. [[CrossRef](#)]
41. Nidheesh, P.V. Graphene-based materials supported advanced oxidation processes for water and wastewater treatment: A review. *Environ. Sci. Pollut. Res. Int.* **2017**, *24*, 27047–27069. [[CrossRef](#)]
42. Londhe, K.; Lee, C.-S.; Zhang, Y.; Grdanovska, S.; Kroc, T.; Cooper, C.A.; Venkatesan, A.K. Energy Evaluation of Electron Beam Treatment of Perfluoroalkyl Substances in Water: A Critical Review. *ACS EST Eng.* **2021**, *1*, 827–841. [[CrossRef](#)]
43. Luo, Y.; Awoyemi, O.S.; Gopalan, S.; Nolan, A.; Robinson, F.; Fenstermacher, J.; Xu, L.; Niu, J.; Megharaj, M.; Naidu, R.; et al. Investigating the effect of polarity reversal of the applied current on electrochemical degradation of per- and polyfluoroalkyl substances. *J. Clean. Prod.* **2023**, *433*, 139691. [[CrossRef](#)]
44. Ilić, N.; Andalib, A.; Lippert, T.; Knoop, O.; Franke, M.; Bräutigam, P.; Drewes, J.E.; Hübner, U. Ultrasonic degradation of GenX (HFPO-DA)—Performance comparison to PFOA and PFOS at high frequencies. *Chem. Eng. J.* **2023**, *472*, 144630. [[CrossRef](#)]
45. Lewis, A.J.; Joyce, T.; Hadaya, M.; Ebrahimi, F.; Dragiev, I.; Giardetti, N.; Yang, J.; Fridman, G.; Rabinovich, A.; Fridman, A.A.; et al. Rapid degradation of PFAS in aqueous solutions by reverse vortex flow gliding arc plasma. *Environ. Sci. Water Res. Technol.* **2020**, *6*, 1044–1057. [[CrossRef](#)]
46. Liu, Z.; Chen, Z.; Gao, J.; Yu, Y.; Men, Y.; Gu, C.; Liu, J. Accelerated Degradation of Perfluorosulfonates and Perfluorocarboxylates by UV/Sulfite + Iodide: Reaction Mechanisms and System Efficiencies. *Environ. Sci. Technol.* **2022**, *56*, 3699–3709. [[CrossRef](#)] [[PubMed](#)]
47. Lee, Y.-C.; Lo, S.-L.; Chiueh, P.-T.; Liou, Y.-H.; Chen, M.-L. Microwave-hydrothermal decomposition of perfluorooctanoic acid in water by iron-activated persulfate oxidation. *Water Res.* **2010**, *44*, 886–892. [[CrossRef](#)] [[PubMed](#)]
48. Ameta, S.; Ameta, R. *Advanced Oxidation Processes for Wastewater Treatment: Emerging Green Chemical Technology*; Academic Press (An Imprint of Elsevier): London, UK, 2018.
49. Moriwaki, H.; Takagi, Y.; Tanaka, M.; Tsuruho, K.; Okitsu, K.; Maeda, Y. Sonochemical Decomposition of Perfluorooctane Sulfonate and Perfluorooctanoic Acid. *Environ. Sci. Technol.* **2005**, *39*, 3388–3392. [[CrossRef](#)]
50. Chen, W.; Zhang, X.; Mamadiev, M.; Wang, Z. Sorption of perfluorooctane sulfonate and perfluorooctanoate on polyacrylonitrile fiber-derived activated carbon fibers: In comparison with activated carbon. *RSC Adv.* **2017**, *7*, 927–938. [[CrossRef](#)]
51. Yasui, K.; Tuziuti, T.; Lee, J.; Kozuka, T.; Towata, A.; Iida, Y. The range of ambient radius for an active bubble in sonoluminescence and sonochemical reactions. *J. Chem. Phys.* **2008**, *128*, 184705. [[CrossRef](#)]
52. Shende, T.; Andaluri, G.; Suri, R. Power density modulated ultrasonic degradation of perfluoroalkyl substances with and without sparging Argon. *Ultrason. Sonochem.* **2021**, *76*, 105639. [[CrossRef](#)]
53. Brotchie, A.; Grieser, F.; Ashokkumar, M. Effect of power and frequency on bubble-size distributions in acoustic cavitation. *Phys. Rev. Lett.* **2009**, *102*, 084302. [[CrossRef](#)]
54. Thompson, L.H.; Doraiswamy, L.K. Sonochemistry: Science and Engineering. *Ind. Eng. Chem. Res.* **1999**, *38*, 1215–1249. [[CrossRef](#)]
55. Beckett, M.A.; Hua, I. Impact of Ultrasonic Frequency on Aqueous Sonoluminescence and Sonochemistry. *J. Phys. Chem. A Mol. Spectrosc. Kinet. Environ. Gen. Theory* **2001**, *105*, 3796–3802. [[CrossRef](#)]
56. Panchangam, S.C.; Lin, A.Y.-C.; Tsai, J.-H.; Lin, C.-F. Sonication-assisted photocatalytic decomposition of perfluorooctanoic acid. *Chemosphere* **2009**, *75*, 654–660. [[CrossRef](#)]
57. Hori, H.; Nagano, Y.; Murayama, M.; Koike, K.; Kutsuna, S. Efficient decomposition of perfluoroether carboxylic acids in water with a combination of persulfate oxidant and ultrasonic irradiation. *J. Fluor. Chem.* **2012**, *141*, 5–10. [[CrossRef](#)]
58. Campbell, T.; Hoffmann, M.R. Sonochemical degradation of perfluorinated surfactants: Power and multiple frequency effects. *Sep. Purif. Technol.* **2015**, *156*, 1019–1027. [[CrossRef](#)]
59. James Wood, R.; Sidnell, T.; Ross, I.; McDonough, J.; Lee, J.; Bussemaker, M.J. Ultrasonic degradation of perfluorooctane sulfonic acid (PFOS) correlated with sonochemical and sonoluminescence characterisation. *Ultrason. Sonochem.* **2020**, *68*, 105196. [[CrossRef](#)] [[PubMed](#)]
60. Shende, T.; Andaluri, G.; Suri, R. Frequency-dependent sonochemical degradation of perfluoroalkyl substances and numerical analysis of cavity dynamics. *Sep. Purif. Technol.* **2021**, *261*, 118250. [[CrossRef](#)]
61. Kanthale, P.; Ashokkumar, M.; Grieser, F. Sonoluminescence, sonochemistry (H<sub>2</sub>O<sub>2</sub> yield) and bubble dynamics: Frequency and power effects. *Ultrason. Sonochem.* **2008**, *15*, 143–150. [[CrossRef](#)] [[PubMed](#)]
62. Hung, H.-M.; Ling, F.H.; Hoffmann, M.R. Kinetics and Mechanism of the Enhanced Reductive Degradation of Nitrobenzene by Elemental Iron in the Presence of Ultrasound. *Environ. Sci. Technol.* **2000**, *34*, 1758–1763. [[CrossRef](#)]
63. Chirikona, F.; Quinete, N.; Gonzalez, J.; Mutua, G.; Kimosop, S.; Orata, F. Occurrence and Distribution of Per- and Polyfluoroalkyl Substances from Multi-Industry Sources to Water, Sediments and Plants along Nairobi River Basin, Kenya. *Int. J. Environ. Res. Public Health* **2022**, *19*, 8980. [[CrossRef](#)]

64. Vecitis, C.D.; Park, H.; Cheng, J.; Mader, B.T.; Hoffmann, M.R. Kinetics and Mechanism of the Sonolytic Conversion of the Aqueous Perfluorinated Surfactants, Perfluorooctanoate (PFOA), and Perfluorooctane Sulfonate (PFOS) into Inorganic Products. *J. Phys. Chem. A Mol. Spectrosc. Kinet. Environ. Gen. Theory* **2008**, *112*, 4261–4270. [[CrossRef](#)]
65. Shende, T.; Andaluri, G.; Suri, R.P.S. Kinetic model for sonolytic degradation of non-volatile surfactants: Perfluoroalkyl substances. *Ultrason. Sonochem.* **2019**, *51*, 359–368. [[CrossRef](#)]
66. Gole, V.L.; Fishgold, A.; Sierra-Alvarez, R.; Deymier, P.; Keswani, M. Treatment of perfluorooctane sulfonic acid (PFOS) using a large-scale sonochemical reactor. *Sep. Purif. Technol.* **2018**, *194*, 104–110. [[CrossRef](#)]
67. Lin, J.-C.; Lo, S.-L.; Hu, C.-Y.; Lee, Y.-C.; Kuo, J. Enhanced sonochemical degradation of perfluorooctanoic acid by sulfate ions. *Ultrason. Sonochem.* **2015**, *22*, 542–547. [[CrossRef](#)] [[PubMed](#)]
68. Lee, Y.-C.; Chen, M.-J.; Huang, C.-P.; Kuo, J.; Lo, S.-L. Efficient sonochemical degradation of perfluorooctanoic acid using periodate. *Ultrason. Sonochem.* **2016**, *31*, 499–505. [[CrossRef](#)] [[PubMed](#)]
69. Vecitis, C.D.; Park, H.; Cheng, J.; Mader, B.T.; Hoffmann, M.R. Enhancement of Perfluorooctanoate and Perfluorooctanesulfonate Activity at Acoustic Cavitation Bubble Interfaces. *J. Phys. Chem. C* **2008**, *112*, 16850–16857. [[CrossRef](#)]
70. Costanza, J.; Arshadi, M.; Abriola, L.M.; Pennell, K.D. Accumulation of PFOA and PFOS at the Air–Water Interface. *Environ. Sci. Technol. Lett.* **2019**, *6*, 487–491. [[CrossRef](#)]
71. Panda, D.; Sethu, V.; Manickam, S. Kinetics and mechanism of low-frequency ultrasound driven elimination of trace level aqueous perfluorooctanesulfonic acid and perfluorooctanoic acid. *Chem. Eng. Process.* **2019**, *142*, 107542. [[CrossRef](#)]
72. Asakura, Y.; Nishida, T.; Matsuoka, T.; Koda, S. Effects of ultrasonic frequency and liquid height on sonochemical efficiency of large-scale sonochemical reactors. *Ultrason. Sonochem.* **2008**, *15*, 244–250. [[CrossRef](#)] [[PubMed](#)]
73. Gogate, P.R.; Sutkar, V.S.; Pandit, A.B. Sonochemical reactors: Important design and scale up considerations with a special emphasis on heterogeneous systems. *Chem. Eng. J.* **2011**, *166*, 1066–1082. [[CrossRef](#)]
74. Hu, Y.-B.; Lo, S.-L.; Li, Y.-F.; Lee, Y.-C.; Chen, M.-J.; Lin, J.-C. Autocatalytic degradation of perfluorooctanoic acid in a permanganate-ultrasonic system. *Water Res.* **2018**, *140*, 148–157. [[CrossRef](#)]
75. Luo, Y.; Khoshyan, A.; Al Amin, M.; Nolan, A.; Robinson, F.; Fenstermacher, J.; Niu, J.; Megharaj, M.; Naidu, R.; Fang, C. Ultrasound-enhanced Magnéli phase Ti(4)O(7) anodic oxidation of per- and polyfluoroalkyl substances (PFAS) towards remediation of aqueous film forming foams (AFFF). *Sci. Total Environ.* **2023**, *862*, 160836. [[CrossRef](#)] [[PubMed](#)]
76. Pétrier, C.; Torres-Palma, R.; Combet, E.; Sarantakos, G.; Baup, S.; Pulgarin, C. Enhanced sonochemical degradation of bisphenol-A by bicarbonate ions. *Ultrason. Sonochem.* **2010**, *17*, 111–115. [[CrossRef](#)] [[PubMed](#)]
77. Cheng, J.; Vecitis, C.D.; Park, H.; Mader, B.T.; Hoffmann, M.R. Sonochemical Degradation of Perfluorooctane Sulfonate (PFOS) and Perfluorooctanoate (PFOA) in Groundwater: Kinetic Effects of Matrix Inorganics. *Environ. Sci. Technol.* **2010**, *44*, 445–450. [[CrossRef](#)] [[PubMed](#)]
78. Yasui, K. Effect of volatile solutes on sonoluminescence. *J. Chem. Phys.* **2002**, *116*, 2945–2954. [[CrossRef](#)]
79. Merouani, S.; Hamdaoui, O.; Saoudi, F.; Chiha, M. Sonochemical degradation of Rhodamine B in aqueous phase: Effects of additives. *Chem. Eng. J.* **2010**, *158*, 550–557. [[CrossRef](#)]
80. Hua, I.; Hoffmann, M.R. Optimization of Ultrasonic Irradiation as an Advanced Oxidation Technology. *Environ. Sci. Technol.* **1997**, *31*, 2237–2243. [[CrossRef](#)]
81. Kewalramani, J.A.; Bezerra de Souza, B.; Marsh, R.W.; Meegoda, J.N. Contributions of reactor geometry and ultrasound frequency on the efficiency of sonochemical reactor. *Ultrason. Sonochem.* **2023**, *98*, 106529. [[CrossRef](#)]
82. Marsh, R.W.; Kewalramani, J.A.; Bezerra de Souza, B.; Meegoda, J.N. The use of a fluorine mass balance to demonstrate the mineralization of PFAS by high frequency and high power ultrasound. *Chemosphere* **2024**, *352*, 141270. [[CrossRef](#)]
83. Shende, T.; Andaluri, G.; Suri, R. Chain-length dependent ultrasonic degradation of perfluoroalkyl substances. *Chem. Eng. J. Adv.* **2023**, *15*, 100509. [[CrossRef](#)]
84. Yang, S.-W.; Sun, J.; Hu, Y.-Y.; Cheng, J.-H.; Liang, X.-Y. Effect of vacuum ultraviolet on ultrasonic defluorination of aqueous perfluorooctanesulfonate. *Chem. Eng. J.* **2013**, *234*, 106–114. [[CrossRef](#)]
85. Sekiguchi, K.; Kudo, T.; Sankoda, K. Combined sonochemical and short-wavelength UV degradation of hydrophobic perfluorinated compounds. *Ultrason. Sonochem.* **2017**, *39*, 87–92. [[CrossRef](#)]
86. Lei, Y.; Zhao, L.; Fang, C.; Naidu, R.; Tian, D.; Zhao, L.; Huang, M.; He, J.; Cheng, Z.; Zeng, Z.; et al. A novel enhanced defluorination of perfluorooctanoic acids by surfactant-assisted ultrasound coupling persulfate. *Sep. Purif. Technol.* **2023**, *317*, 123906. [[CrossRef](#)]
87. Lei, Y.; Pu, R.; Tian, Y.; Wang, R.; Naidu, R.; Deng, S.; Shen, F. Novel enhanced defluorination of perfluorooctanoic acids by biochar-assisted ultrasound coupling ferrate: Performance and mechanism. *Bioresour. Technol.* **2024**, *402*, 130790. [[CrossRef](#)]
88. Gole, V.L.; Sierra-Alvarez, R.; Peng, H.; Giesy, J.P.; Deymier, P.; Keswani, M. Sono-chemical treatment of per- and poly-fluoroalkyl compounds in aqueous film-forming foams by use of a large-scale multi-transducer dual-frequency based acoustic reactor. *Ultrason. Sonochem.* **2018**, *45*, 213–222. [[CrossRef](#)] [[PubMed](#)]
89. Kewalramani, J.A.; Wang, B.; Marsh, R.W.; Meegoda, J.N.; Rodriguez Freire, L. Coupled high and low-frequency ultrasound remediation of PFAS-contaminated soils. *Ultrason. Sonochem.* **2022**, *88*, 106063. [[CrossRef](#)]
90. Kulkarni Poonam, R.; Richardson Stephen, D.; Nzeribe Blossom, N.; Adamson David, T.; Kalra Shashank, S.; Mahendra, S.; Blotevogel, J.; Hanson, A.; Dooley, G.; Maravirov, S.; et al. Field Demonstration of a Sonolysis Reactor for Treatment of PFAS-Contaminated Groundwater. *J. Environ. Eng.* **2022**, *11*, 06022005. [[CrossRef](#)]



91. Laramay, F.; Crimi, M. Theoretical evaluation of chemical and physical feasibility of an in situ ultrasonic reactor for remediation of groundwater contaminated with per- and polyfluoroalkyl substances. *Remediation* **2020**, *1*, 45–58. [[CrossRef](#)]
92. Zhang, W.; Zhang, Q.; Liang, Y. Ineffectiveness of ultrasound at low frequency for treating per- and polyfluoroalkyl substances in sewage sludge. *Chemosphere* **2022**, *286*, 131748. [[CrossRef](#)]

**Disclaimer/Publisher’s Note:** The statements, opinions and data contained in all publications are solely those of the individual author(s) and contributor(s) and not of MDPI and/or the editor(s). MDPI and/or the editor(s) disclaim responsibility for any injury to people or property resulting from any ideas, methods, instructions or products referred to in the content.